AGU PUBLICATIONS

Geophysical Research Letters

RESEARCH LETTER
10.1002/2015GL065237

Key Points:
- Satellite observations show distinct short-term mesospheric HO_2 variability
- HO_2 variability correlates well with solar UV changes during 27 day cycles

Supporting Information:
- Supporting Information S1
- Data Set S1

Correspondence to:
S. Wang,
Shuhui.Wang@jpl.nasa.gov

Citation:
Wang, S., Q. Zhang, L. Millán, K.-F. Li, Y. L. Yung, S. P. Sander, N. J. Livesey, and M. L. Santee (2015), First evidence of middle atmospheric HO_2 response to 27 day solar cycles from satellite observations, *Geophys. Res. Lett.*, *42*, 10,004–10,009, doi:10.1002/2015GL065237.

Received 6 JUL 2015
Accepted 12 OCT 2015
Accepted article online 14 OCT 2015
Published online 16 NOV 2015

©2015. American Geophysical Union. All Rights Reserved.

First evidence of middle atmospheric HO_2 response to 27 day solar cycles from satellite observations

Shuhui Wang[1], Qiong Zhang[2], Luis Millán[1], King-Fai Li[3], Yuk L. Yung[2], Stanley P. Sander[1], Nathaniel J. Livesey[1], and Michelle L. Santee[1]

[1]Jet Propulsion Laboratory, California Institute of Technology, Pasadena, California, USA, [2]Division of Geological and Planetary Sciences, California Institute of Technology, Pasadena, California, USA, [3]Department of Applied Mathematics, University of Washington, Seattle, Washington, USA

Abstract HO_2 and OH, also known as HO_x, play an important role in controlling middle atmospheric O_3. Due to their photochemical production and short chemical lifetimes, HO_x are expected to respond rapidly to solar irradiance changes, resulting in O_3 variability. While OH solar cycle signals have been investigated, HO_2 studies have been limited by the lack of reliable observations. Here we present the first evidence of HO_2 variability during solar 27 day cycles by investigating the recently developed HO_2 data from the Aura Microwave Limb Sounder (MLS). We focus on 2012–2015, when solar variability is strong near the peak of Solar Cycle 24. The features of HO_2 variability, with the strongest signals at 0.01–0.068 hPa, correlate well with those of solar Lyman α. When continuous MLS OH observations are not available, the new HO_2 data could be a promising alternative for investigating HO_x variability and the corresponding impacts on O_3 and the climate.

1. Introduction

The odd hydrogen species (HO_x) are well known for their role in the catalytic destruction of middle atmospheric O_3. In particular, above ~40 km, the major catalytic O_3 loss is controlled by HO_x reaction cycles involving OH, HO_2, and atomic hydrogen (H) [e.g., *Wang et al.*, 2013], where X = OH/H and XO = HO_2/OH.

$$X + O_3 \rightarrow XO + O_2 \quad (1)$$

$$O + XO \rightarrow O_2 + X \quad (2)$$

The net result of these reaction cycles is the removal of two odd oxygen species, O_3 and atomic oxygen (O), without changing the abundance of HO_x.

$$O + O_3 \rightarrow 2O_2 \quad (\text{net result of (1) and (2)}) \quad (3)$$

The main sources of HO_x during daytime are photolysis of H_2O (mainly in the mesosphere),

$$H_2O + h\nu \rightarrow OH + H \quad (\sim 121 \text{ nm; } 175\text{–}205 \text{ nm}) \quad (4)$$

and of O_3 (mainly in the stratosphere) [e.g., *Brasseur and Solomon*, 2005].

$$O_3 + h\nu \rightarrow O_2 + O(^1D) \quad (200\text{–}330 \text{ nm}) \quad (5)$$

$$O(^1D) + H_2O \rightarrow 2OH \quad (6)$$

The termination of the reaction cycles is the ultimate removal of HO_x through self-reactions, e.g., reaction (7).

$$OH + HO_2 \rightarrow H_2O + O_2 \quad (7)$$

Due to their photochemical production, HO_x abundances vary with solar UV irradiance over various time scales and magnitudes. They exhibit distinct diurnal [e.g., *Li et al.*, 2005; *Minschwaner et al.*, 2011] and seasonal [e.g., *Canty and Minschwaner*, 2002] variabilities. Moreover, OH has been shown to vary with solar cycles (the 11 year cycle [*Wang et al.*, 2013] and the 27 day cycle [*Shapiro et al.*, 2012]). It has been suggested that the solar 11 year cycle variability in OH and the corresponding HO_x chemistry dominate O_3 solar cycle variability above 40 km [*Wang et al.*, 2013].

While O_3 responses to natural solar forcing are important for understanding the Sun-climate interaction, large disagreements in O_3 solar cycle signals among various observations and between models and observations

remain unresolved, making it challenging to evaluate how well climate models simulate natural O_3 variability and predict future O_3 layer changes [e.g., *Haigh et al*., 2010; *Merkel et al*., 2011; *Swartz et al*., 2012; *Ermolli et al*., 2013; *Solanki et al*., 2013; *Ball et al*., 2014a]. In particular, the large discrepancies in solar spectral irradiance (SSI) variability during 11 year cycles result in huge uncertainties in climate model results [e.g., *Lean and Deland*, 2012; *Fontenla et al*., 2011; *Ball et al*., 2014b; *Morrill et al*., 2014; *Thuillier et al*., 2014]. While O_3 responses to solar forcing are complex, involving direct (O_3 photolysis) and various indirect effects (e.g., through photochemical variability in HO_x, dynamics, and atmospheric heating), in the middle atmosphere they are mostly through photochemistry [*Swartz et al*., 2012], in particular HO_x chemistry above 40 km [*Wang et al*., 2013]. Given the short HO_x chemical lifetime and the relative simplicity of HO_x variability, quantifying and understanding HO_x variability could be the steppingstone that leads to a better understanding of O_3 changes. Therefore, evidence of solar-induced HO_x variability is an important input to investigations of the corresponding solar impacts on O_3 and climate. Since the uncertainty in SSI variability is rather small for short-term solar forcing (i.e., 27 day cycles) [*Deland and Cebula*, 2012; *Lean and Deland*, 2012], quantifying HO_x variability during 27 day solar cycles could be the first step in understanding solar forcing impacts on middle atmospheric HO_x chemistry.

While OH solar 27 day cycle signals have been reported based on satellite observations [*Shapiro et al*., 2012], little attention has been paid to HO_2, which also plays an important role in HO_x reaction cycles. The main reason is the lack of reliable HO_2 data with the required quality. The recently developed HO_2 data from the Aura Microwave Limb Sounder (MLS) make it possible, for the first time, to investigate the subtle signals of solar-induced HO_2 variability.

2. Data

2.1. Aura MLS HO_2 Data

MLS was launched in July 2004 on the Sun-synchronous Aura satellite. The crossing time at the equator is ~13:45 for daytime (ascending parts of the orbit) and ~1:45 for nighttime (descending). MLS provides the first long-term continuous global daily vertical profile data for OH and HO_2 for both day and night [e.g., *Pickett et al*., 2008]. OH is measured with the THz subinstrument, while HO_2 and all other species are measured with GHz radiometers. Continuous daily OH measurements are available from August 2004 to December 2009. Due to aging of the THz subinstrument, after 2009, OH data are only available for ~30 day periods every summer since 2011. Daily measurements of MLS HO_2 are continuing and currently provide the only available long-term global data set for HO_2. Other space-borne HO_2 data are only available for short intervals and/or during periods when solar activity is moderate or weak (e.g., data from the submillimeter radiometer on Odin during October 2003 to December 2005 [*Baron et al*., 2009] and from the Superconducting Submillimeter-Wave Limb Emission Sounder during October 2009 to April 2010 [*Kikuchi et al*., 2010]).

While the MLS HO_2 data record is over 10 years long and covers the current 11 year solar cycle peak (Solar Cycle 24), the original standard MLS HO_2 data [*Livesey et al*., 2015] lack the accuracy and stability needed for studying the subtle solar cycle variability. Recently, an "off-line" version of the MLS HO_2 data product, with significantly improved quality, has been developed, bringing a brand new opportunity [*Millán et al*., 2015]. This new retrieval is based on daily zonal mean radiances in 10° latitude bins. It has a wide global coverage of 82°S–82°N, with a vertical range of 10–0.003 hPa, which allows for investigations of mesospheric trends and variability. To further reduce the noise and to minimize the effect of strong seasonal cycles, we focus on "global mean" data in a wide latitude range of 55°S–55°N. An overview of daytime off-line HO_2 data (10.5 years) is shown in Figure 1. The mesospheric HO_2 density peak occurs at ~70 km (~0.046 hPa). The HO_2 abundance also clearly increases from the solar minimum in 2008–2009 to the recent solar maximum in 2012–2015 as solar UV irradiance increases with the 11 year cycle.

2.2. Solar Lyman-Alpha Data

Solar Lyman α (~121.5 nm) has been widely used as an index for solar UV irradiance. Water vapor (H_2O) photolysis at the Lyman α wavelength is a major source of mesospheric HO_x. We use the Lyman α long-term composite from LISIRD: Laboratory for Atmospheric and Space Physics (LASP) Interactive Solar Irradiance Data Center (http://lasp.colorado.edu/lisird/). This composite covers multiple solar 11 year cycles and includes observations from six satellite instruments and various models to fill in gaps between measurements. The

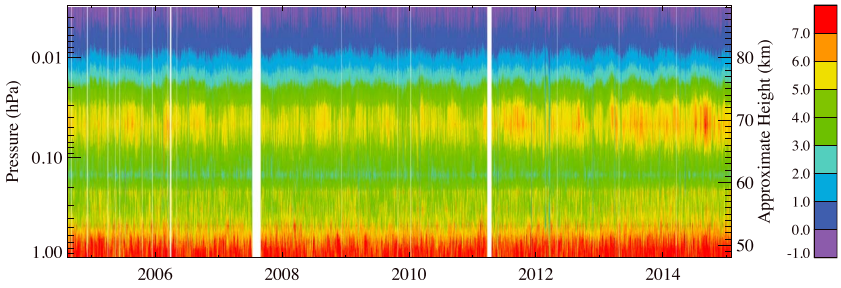

Figure 1. Overview of daytime global mean (55°S–55°N) data of MLS off-line HO_2 (10^6 cm^{-3}). Gaps are missing data.

values are all scaled to match the UARS reference level as discussed by *Woods et al.* [2000]. For the most recent decade, data are from the Solar Stellar Irradiance Comparison Experiment on board NASA's Solar Radiation and Climate Experiment, launched in 2003, and the EUV Variability Experiment on board NASA's Solar Dynamics Observatory, launched in 2010.

Figure 2a shows the Lyman α time series from January 2004 to February 2015. The black line shows the daily data, and the cyan line (36 day fast Fourier transform (FFT) smoothing) indicates the trend or "baseline" that is not associated with 27 day cycles. A 36 day window for smoothing was chosen based on earlier studies of OH variability [*Shapiro et al.*, 2012], which found that a 20–35 day band-pass filter can satisfactorily extract the solar 27 day cycle signal. The Lyman α trend generally follows the solar 11 year cycle, decreasing from 2004 to 2009 and increasing thereafter. When the original daily data are normalized to the baseline, the short-term oscillation, which is mostly due to the 27 day cycles, is clearly demonstrated (Figure 2b). The most recent three years (2012–2015) show the strongest 27 day cycle variability in solar UV and thus represent the best time period for investigating the subtle changes in atmospheric HO_2. Therefore, our data analysis is focused on these three years.

3. Results and Discussion

To extract the 27 day variability signal due to solar cycles, both longer-term variability (primarily consisting of the seasonal cycle, solar 11 year cycle, and the trend) and the day-to-day noise have to be removed. While previous studies used a simple 20–35 day band-pass filter to extract the solar 27 day cycle signal [*Shapiro et al.*, 2012], we use a different method that is less likely to introduce artificial oscillations through numerical filters. Using 0.032 hPa data as an example, Figure 3 illustrates the methodology for removing the longer-term variability and the day-to-day noise. We first applied a 36 day FFT smoothing to the daily HO_2 data (after eliminating outliers using a criterion of 3 times the standard deviation and filling gaps with linear interpolation). The resulting longer-term trend was used as the baseline (Figure 3a, cyan). The original daily HO_2 data were then normalized to the baseline to calculate the percentage variation from it (Figure 3b, cyan). After another round of outlier removal (>3 times the standard deviation), a 10 day FFT smoothing was then applied to further smooth out the day-to-day noise (Figure 3b, blue). The resulting variability should be mostly associated with the 27 day solar cycles. The same steps were also applied to the

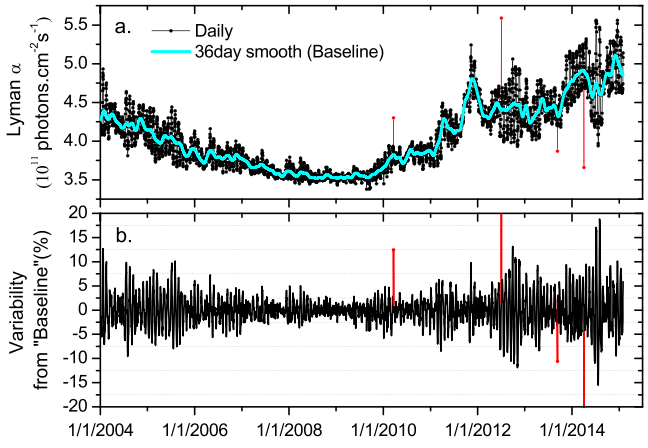

Figure 2. (a) The time series of daily Lyman α data from January 2004 to February 2015 (black) and the trend baseline (cyan: 36 day FFT smoothing); (b) The short-term variability from the baseline calculated by normalizing daily data to the baseline value. The red points indicate outliers that are out of the range of 3 times standard deviations.

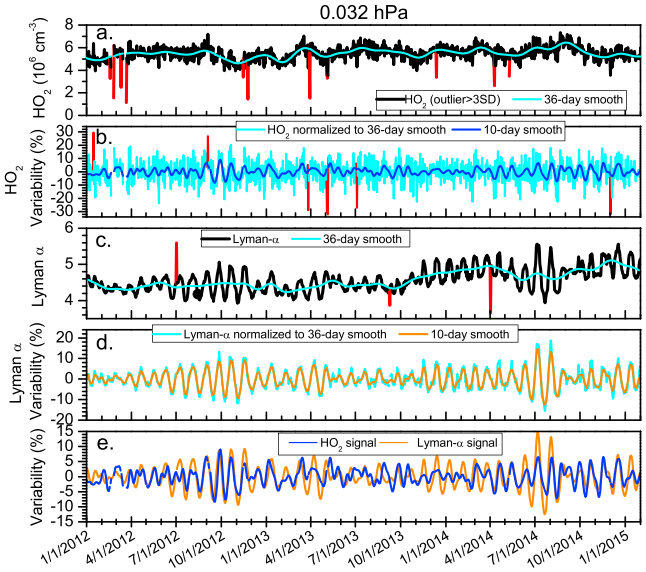

Figure 3. The 27 day solar cycle variability in HO_2 and Lyman α at 0.032 hPa. (a) The global mean (55°S–55°N) MLS HO_2 daily data (black) and the 36 day FFT smoothing result (cyan), which is used as the "baseline" trend. The red points are considered outliers (using 3 times the standard deviation as the threshold) and excluded from the analysis. (b) The original daily HO_2 data are normalized to the baseline value (cyan) and then smoothed by applying a 10 day smoothing to remove the day-to-day noise (blue). (c and d) are the same as Figures 3a and 3b except that the data are for Lyman α instead of HO_2. The unit of Lyman α data is as shown in Figure 2. (e) The comparison of variability in HO_2 and Lyman α during solar 27 day cycles.

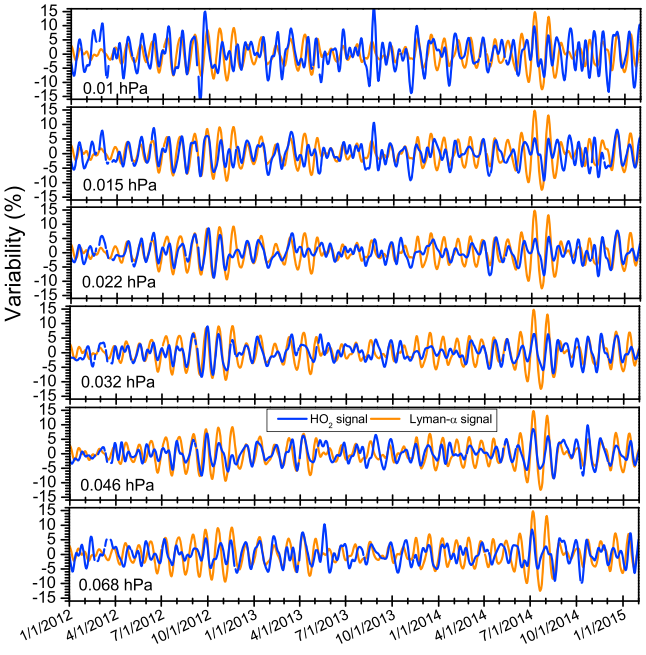

Figure 4. Signatures of solar 27 day cycle variability in MLS HO_2 data at six pressure levels in the mesosphere. Note that the Lyman α variability signal shown in all panels is the same because the LISIRD Lyman α data are for the top of the atmosphere rather than the irradiance penetrating into each layer of the atmosphere.

daily Lyman α data (Figures 3c and 3d). The resulting "fingerprint" features of the variability in HO_2 and Lyman α correlate with each other very well (Figure 3e), including the times when Lyman α oscillations are somewhat weak or irregular.

We extended the analysis to all other pressure levels for which MLS HO_2 data are available. As shown in Figure 4, clearly defined 27 day cycle signals were found at all six pressure levels between 0.01 hPa and 0.068 hPa, which cover the entire mesospheric HO_2 density peak (see Figure 1). At lower altitudes ($\geq$0.1 hPa), the penetrating solar UV irradiance is greatly reduced and thus the signatures of solar cycle variability in HO_2 become noisier. At higher altitudes ($\leq$0.0068 hPa), HO_2 density is too small and HO_2 data become too noisy for extracting solar cycle signals, although the percentage HO_2 variability is likely larger due to stronger penetrating solar UV irradiance. For all six pressure levels, the cross correlation analysis indicates that HO_2 and Lyman α variabilities correlate with each other with no significant time lag (Figure S1 in the supporting information).

The linear regression between HO_2 variability and Lyman α variability is a measure of HO_2 response to solar UV changes. The linear fit plots are included in supporting information (Figure S2 and Table S1 in the supporting information). The slope of the fit quantifies HO_2 sensitivity to Lyman α changes (% variability in HO_2 due to 1% variability in Lyman α). Figure 5 summarizes the HO_2 sensitivity at all pressure levels. The blue line shows the goodness of the fit (correlation coefficient R^2).

This vertical profile of HO_2 sensitivity to solar Lyman α changes has a peak at 0.032–0.046 hPa (~70–75 km), which is close to but slightly higher than that of the HO_2 density peak in the mesosphere. The altitude of the strongest HO_2 solar cycle signals should be a compromise between the decreasing HO_2 abundances and the increasing

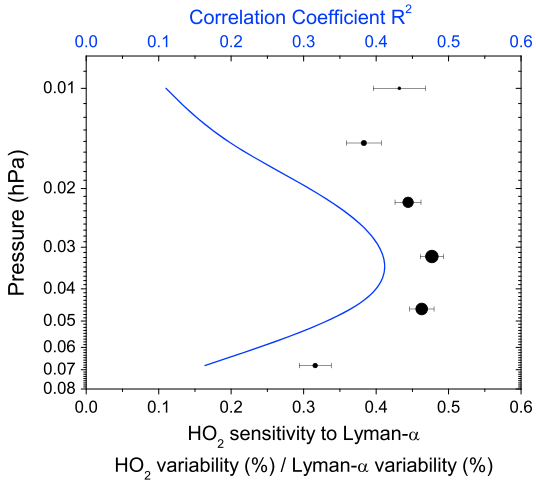

Figure 5. Vertical profile of MLS HO_2 sensitivity to solar Lyman α variability (measured by the slope of linear fits between variabilities in HO_2 and Lyman α). The size of the error bars represents the uncertainty in the linear fit. The correlation coefficient R^2 is plotted in blue and also reflected in the size of the symbols.

penetrating UV irradiance with altitude. It is thus not surprising to see the peak HO_2 variability signal occur at an altitude higher than that of the HO_2 density peak. Whether the HO_2 solar cycle signal continues to increase above the altitude of 0.01 hPa (as suggested by the OH solar cycle signal study of *Shapiro et al.* [2012]) cannot be confirmed with MLS HO_2 data.

HO_2 data during the earlier years of Aura MLS (2004–2005), when solar activity was moderate (in the middle of the declining phase of Solar Cycle 23), were also analyzed. Similar signatures of HO_2 variability with Lyman α are also seen, but the correlations are weaker (only one pressure level has R^2 greater than 0.3; see Figure S3 in the supporting information). We also applied the same analysis to the entire MLS measurement record (2004–2015). However, due to the weak solar activity and thus weak solar 27 day cycles (as shown in Figure 2b), no significant HO_2 27 day variability was found during most of the period from 2006 to 2011. Furthermore, we extended the analysis to nighttime HO_2 data and, as expected, found no correlation between HO_2 and Lyman α. These results demonstrate the robustness of our analysis.

The band-pass filter used in earlier OH studies [*Shapiro et al.*, 2012] was also used for our HO_2 variability analysis. The results are similar to those extracted using the aforementioned technique, except that the slopes from the band-pass filter analysis are often larger than the results in Figure 5 with larger error bars and the linear correlations are mostly worse (see Table S1).

4. Summary

By analyzing the recently developed off-line Aura MLS HO_2 data, we found the first evidence of global mean HO_2 variability during solar 27 day cycles. The distinct features of mesospheric HO_2 variability are shown to correlate well with those of solar Lyman α variability. The strongest HO_2 solar cycle signals were found in the pressure range of 0.01–0.068 hPa during 2012–2015. While continuous observations of MLS OH are not available after the end of 2009, the new HO_2 data are a promising alternative for investigating HO_x variability. Quantifying and understanding the solar forcing impacts on middle atmospheric O_3-controlling HO_x species will enable better understanding of the more complex solar-induced changes in O_3 and the climate.

Acknowledgments
We acknowledge the support of the NASA Aura Science Team, Upper Atmosphere Research, and Tropospheric Chemistry programs. Work at the Jet Propulsion Laboratory, California Institute of Technology, was done under contract to the National Aeronautics and Space Administration. We acknowledge the LASP Interactive Solar Irradiance Datacenter (LISIRD) for Lyman α record (http://lasp.colorado.edu/lisird/).

References

Ball, W. T., D. J. Mortlock, J. S. Egerton, and J. D. Haigh (2014a), Assessing the relationship between spectral solar irradiance and stratospheric ozone using Bayesian inference, *J. Space Weather Space Clim.*, *4*, A25, doi:10.1051/swsc/2014023.

Ball, W. T., N. A. Krivova, Y. C. Unruh, J. D. Haigh, and S. K. Solanki (2014b), A New SATIRE-S spectral solar irradiance reconstruction for solar cycles 21–23 and its implications for stratospheric ozone, *J. Atmos. Sci.*, *71*, 4086–4101, doi:10.1175/JAS-D-13-0241.1.

Baron, P., E. Dupuy, J. Urban, D. P. Murtagh, P. Eriksson, and Y. Kasai (2009), HO_2 measurements in the stratosphere and the mesosphere from the sub millimeter limb sounder Odin/SMR, *Int. J. Remote. Sens.*, *30*(15–16), 4195–4208.

Brasseur, G. P., and S. Solomon (2005), *Aeronomy of the Middle Atmosphere: Chemistry and Physics of the Stratosphere and Mesosphere*, 3rd ed., 646 pp., Springer, Dordrecht, Netherlands.

Canty, T., and K. Minschwaner (2002), Seasonal and solar cycle variability of OH in the middle atmosphere, *J. Geophys. Res.*, *107*(D24), 4737, doi:10.1029/2002JD002278.

Deland, M. T., and R. P. Cebula (2012), Solar UV variations during the decline of Cycle 23, *J. Atmos. Sol. Terr. Phys.*, *77*, 225–234.

Ermolli, I., et al. (2013), Recent variability of the solar spectral irradiance and its impact on climate modeling, *Atmos. Chem. Phys.*, *13*, 3945–3977, doi:10.5194/acp-13-3945-2013.

Fontenla, J. M., J. Harder, W. Livingston, M. Snow, and T. Woods (2011), High-resolution solar spectral irradiance from extreme ultraviolet to far infrared, *J. Geophys. Res.*, *116*, D20108, doi:10.1029/2011JD016032.

Haigh, J. D., A. R. Winning, R. Toumi, and J. W. Harder (2010), An influence of solar spectral variations on radiative forcing of climate, *Nature*, *467*(7316), 696–699, doi:10.1038/nature09426.

Kikuchi, K., et al. (2010), Overview and early results of the Superconducting Submillimeter-Wave Limb-Emission Sounder (SMILES), *J. Geophys. Res.*, *115*, D23306, doi:10.1029/2010JD014379.

Lean, J. L., and M. T. Deland (2012), How does the Sun's spectrum vary?, *J. Clim.*, *25*, 2555–2560.

Li, K. F., R. P. Cageao, E. M. Karpilovsky, F. P. Mills, Y. L. Yung, J. S. Margolis, and S. P. Sander (2005), OH column abundance over Table Mountain Facility, California: AM-PM diurnal asymmetry, *Geophys. Res. Lett.*, *32*, L13813, doi:10.1029/2005GL022521.

Livesey, N. J., et al. (2015), Earth Observing System (EOS) Microwave Limb Sounder (MLS) Version 4.2x Level 2 data quality and description document *Report JPL D-33509*, Jet Propul. Lab., California Inst. Technol., Pasadena, Calif.

Merkel, A. W., J. W. Harder, D. R. Marsh, A. K. Smith, J. M. Fontenla, and T. N. Woods (2011), The impact of solar spectral irradiance variability on middle atmospheric ozone, *Geophys. Res. Lett.*, *38*, L13802, doi:10.1029/2011GL047561.

Millán, L., S. Wang, N.z. Livesey, H. Sagawa, and Y. Kasai (2015), Stratospheric and mesospheric HO_2 observations from the Aura Microwave Limb Sounder, *Atmos. Chem. Phys.*, *15*, 2889–2902, doi:10.5194/acp-15-2889-2015.

Minschwaner, K., G. L. Manney, S. Wang, and R. S. Harwood (2011), Hydroxyl in the stratosphere and mesosphere—Part 1: Diurnal variability, *Atmos. Chem. Phys.*, *11*, 955–962, doi:10.5194/acp-11-955-2011.

Morrill, J. S., L. Floyd, and D. McMullin (2014), Comparison of solar UV spectral irradiance from SUSIM and SORCE, *Solar Phys.*, doi:10.1007/s11207-014-0535-5.

Pickett, H. M., et al. (2008), Validation of Aura Microwave Limb Sounder OH and HO_2 measurements, *J. Geophys. Res.*, *113*, D16S30, doi:10.1029/2007JD008775.

Shapiro, A. V., E. Rozanov, A. I. Shapiro, S. Wang, T. Egorova, W. Schnutz, and T. Peter (2012), Signature of the 27-day solar rotation cycle in mesospheric OH and H_2O observed by the Aura Microwave Limb Sounder, *Atmos. Chem. Phys.*, *12*, 3181–3188, doi:10.5194/acp-12-3181-2012.

Solanki, S. K., N. A. Krivova, and J. D. Haigh (2013), Solar irradiance variability and climate, *Annu. Rev. Astron. Astrophys.*, *51*, doi:10.1146/annurev-astro-082812-141007.

Swartz, W. H., R. S. Stolarski, L. D. Oman, E. L. Fleming, and C. H. Jackman (2012), Middle atmosphere response to different descriptions of the 11-yr solar cycle in spectral irradiance in a chemistry-climate model, *Atmos. Chem. Phys.*, *12*, 5937–5948, doi:10.5194/acp-12-5937-2012.

Thuillier, G., et al. (2014), Analysis of different solar spectral irradiance reconstructions and their impact on solar heating rates, *Solar Phys.*, *289*, 1115–1142.

Wang, S., et al. (2013), Atmospheric OH response to the most recent 11-year solar cycle, *Proc. Natl. Acad. Sci. U.S.A.*, doi:10.1073/pnas.1117790110.

Woods, T. N., W. K. Tobiska, G. J. Rottman, and J. R. Worden (2000), Improved solar Lyman α irradiance modeling from 1947 through 1999 based on UARS observations, *J. Geophys. Res.*, *105*(A12), 27,195–27,215, doi:10.1029/2000JA000051.